Electronic Supplementary Material (ESI) for ChemComm.

Supplementary Information

Reversing tumor multidrug resistance with a catalytically active covalent organic framework

Peng Gao,‡ Teng Zheng,‡ Bingjie Cui, Xiaohan Liu, Wei Pan,* Na Li, and Bo Tang*

College of Chemistry, Chemical Engineering and Materials Science, Key Laboratory of Molecular and Nano Probes, Ministry of Education, Collaborative Innovation Center of Functionalized Probes for Chemical Imaging in Universities of Shandong, Institute of Molecular and Nano Science, Shandong Normal University, Jinan 250014, P. R. China.

*E-mail: panwei@sdnu.edu.cn; tangb@sdnu.edu.cn.

Table of Contents

1. Reagents and Materials.

5,10,15,20-tetrakis(4-aminophenyl)-21H,23H-porphine (Tph) and 2,5-dihydroxyterephthalaldehyde (Dha) were obtained from Changchun Third Party Pharmaceutical Technology Co. Ltd. 3-(4,5-dimethylthiazol-2-yl)-2,5-diphenyltetrazolium bromide (MTT) was purchased from Sigma Chemical Company. Calcein-AM/PI Double Stain Kit, Annexin V-FITC Apoptosis Detection Kit were purchased from Beyotime (Nantong, China). $FeCl_2 \cdot 4H_2O$ was purchased from Tianjin Dingsheng Xin Chemical Co., Ltd. Confocal dish was purchased from Cellvis, Mountain View, CA. Methylene blue (MB), 2, 2'-azino-bis(3-ethylbenzothiazoline-6-sulfonic acid) (ABTS) were purchased from Shanghai McLean Biochemical Technology Co., Ltd. DMF, THF, DMSO, acetone, methanol and H_2O_2 solution (30 %) were purchased from China National Pharmaceutical Group Corporation (Shanghai, China). All the other chemical reagents were of analytical grade and used without further purification.

2. Apparatus.

Fourier infrared spectrometer (Nicolet iS50 FT-IR) was used to characterize the infrared spectrum. Powder X-ray diffraction (XRD) pattern was obtained on a Rigaku SmartLab SE X-Ray Powder Diffractometer with Cu Kα line focused radiation (λ = 1.5405 Å). Transmission electron microscopy (TEM, HT7700, Japan) was carried out to characterize the morphology of the nanoparticles. UV-vis spectroscopy was achieved with UV-1700 (Shimadzu, Japan). Fluorescence spectra were obtained using a FLS-980 Edinburgh Fluorescence Spectrometer with a Xenon lamp. The absorbance was measured in a microplate reader (Synergy 2, Biotek, USA) for the MTT assay. Confocal fluorescence imaging studies were performed using a TCS SP8 confocal laser scanning microscope (Leica, Germany). All pH measurements were performed with a digital pH-meter (pH-3e, LeiCi, China). Imaging flow cytometry was accomplished on Amnis ImageStream MarkII (Merck Millipore, Seattle, WA). *In vivo* fluorescence images were captured using live animal imaging system (IVIS Lumina III, US).

3. Experimental methods

Preparation of COF NPs. The porphyrin COF was prepared by mixing Dha (15 mg, 0.09 mmol) and Tph (30.5 mg, 0.045 mmol) in dichlorobenzene/butyl alcohol/6 M acetic acid (5/5/1, v/v/v, 2.6 mL). After sonication for 10 min, the mixture was degassed in a Pyrex tube (20 mL) through freeze-pump-thaw cycles for three times and then sealed off. The tube was heated 3 days at 120 °C. After that, the product was collected and washed with THF, acetone. The COF NPs was prepared by disperse COF into DMF followed by sonication for 30 min and further collected *via* differential centrifugation (4000 rpm for 10 min, collect the supernatant to remove large COF, and 10000 rpm, 20 min, collect the precipitation to obtain the nanoscale COF NPs).

Preparation of COF(Fe). 2 mg COF NPs and 5 mg $FeCl_2 \cdot 4H_2O$ were mixed in 2 mL DMF, the solution was refluxed in argon atmosphere for 4 h. The final mixtures were centrifuged at 14500 rpm and washed twice with DMF and twice with methanol to obtain the COF(Fe).

Preparation of COF@DOX and COF(Fe)@DOX. 1 mg of COF and 2 mg of DOX were mixed in 1 mL of aqueous solution in dark for 48 h. Then the above solution was centrifuged at 14000 rpm. The precipitate was washed twice with deionized water. The supernatant was collected to calculate the drug loading efficiency according to the standard curves. COF(Fe)@DOX was prepared by the same procedure except COF NPs were displaced by COF(Fe).

Detection the generation of •OH. ABTS and MB were employed to determine the ·OH generation. For ABTS assay, ABTS was added into the COF and COF(Fe) solutions (0.5 mg/mL) with or without H_2O_2. After incubated for 60 min, the solutions were centrifugated and the UV-Vis absorbance spectra of the supernatants were detected. For MB degradation assay, the same procedure was performed excepted that the ABTS was replaced by the MB.

Calculation the DOX loading efficiency of COF and COF(Fe). Different weights of DOX were added to the 1 mg/mL solutions of COF and COF (Fe) and stirred under dark for 48 h. Then, the fluorescence spectra of DOX in the supernatant

was detected after collected by centrifugation (14000 rpm, 10 min). According to the fluorescence standard curve, the corresponding concentration of DOX in the supernatant was calculated. The loading rate was calculated by [(m_{DOX}-$m_{DOX\ supernatant}$)/m_{DOX}×100%)]. The loading capacity was calculated by [$m_{DOX\ loaded}$/$m_{COF/COF(Fe)}$].

Cell culture. MCF-7/Adr cells were cultured in 1640 medium containing DOX (1 μg/mL). The culture media containing 10 % (V/V) of fetal bovine serum and 100 U/mL of 1% penicillin/streptomycin. The cells were cultured in an incubator containing 5% CO_2 at 37 °C.

Confocal imaging. In order to evaluate the ·OH generation effect of the nanocarriers in cells, coumarin was used to detect the intracellular level of ·OH. MCF-7/Adr cells were cultured in confocal dishes for 24 h. PBS, DOX, COF, COF(Fe), COF@DOX, and COF(Fe)@DOX were then added to the confocal dishes, respectively. (DOX: 0.073 mg/mL, NPs: 0.1 mg/mL) After incubation at 37 °C for 6 h, coumarin was added into the confocal dishes for 2 h. Then the cells were washed with PBS twice and imaged by confocal imaging system to monitor the fluorescence of hydroxycoumarin in cells.

Confocal imaging was performed to investigate the intracellular DOX accumulation in MCF-7/Adr cancer cells with different treatments. MCF-7/Adr cells were cultured in confocal dishes for 24 h. Then, DOX, COF@DOX and COF(Fe)@DOX were added into the cells respectively (DOX: 0.073 mg/mL, NPs: 0.1 mg/mL), and incubated at 37 °C for 6 h. Then the culture solutions were replaced by fresh culture medium and incubated for another 12 h. Finally, the cells were washed with PBS and imaged on a laser scanning confocal microscope.

Flow cytometry analysis. MCF-7/Adr cells were cultured in cell dishes for 24 h. The cells were divided into 3 groups: I: DOX, II: COF@DOX, III: COF(Fe)@DOX (DOX: 0.073 mg/mL, NPs: 0.1 mg/mL). After incubated with different agents for 6 h, the cells were washed with PBS and further cultured for another 6 h. Finally, the cells were washed with PBS thrice and collected and analyzed by flow cytometry.

To evaluate the anticancer cell effect of the nanocarriers, cells were cultured in cell dishes for 24 h. The cells were divided into 6 groups: I: PBS, II: COF, III: DOX, IV: COF(Fe), V: DOX@COF, VI: DOX@COF(Fe) (DOX: 0.073 mg/mL, NPs: 0.1 mg/mL). After adding different agents, all the cells were further cultured for another 24 h. Subsequently, the cells were washed with PBS thrice and treated with Annexin V-FITC/PI for 20 min. Then the cells were analyzed by flow cytometry.

MTT assay. To identify the cell inhibition effect of different materials, MTT assay was performed. The MCF-7/Adr cells were incubated in 96-well plates and cultured for 24 h. The cells were divided into 6 groups: PBS, Dox, COF, COF(Fe), DOX@COF and COF(Fe)@DOX. Different agents with various concentrations were added into the wells respectively. After incubated at 37 °C for 6 h, these solutions were replaced with fresh culture medium and further incubated for 48 h. Finally, the culture medium was sucked out and 200 μL of MTT solution (0.5 mg/mL) was added into each well and incubated for another 4 h. After removing the solutions, formazan crystals in cells were dissolved in 200 μL dimethyl sulfoxide (DMSO), and the absorbance at 490 nm was measured with an microplate reader.

Tumor Models Establishment. All animal experiments were conducted and agreed with the Principles of Laboratory Animal Care (People's Republic of China) and the Guidelines of the Animal Investigation Committee, Biology Institute of Shandong Academy of Science, China. Nude mice (8 weeks old, female, ~20 g) were fed with normal conditions of 12 h light and dark cycles and given access to food and water ad libitum. 1×10^7 MCF-7/Adr cells were injected subcutaneously into the right axillary region of the nude mice. After the tumor size had reached approximately 75-100 mm^3, the mice were used in subsequent experiments.

In *vivo* drug release effect. To investigate the in *vivo* release and distribution of DOX in different groups, 50 μL of DOX, COF@DOX and COF(Fe)@DOX solutions were intratumorally injected into the MCF-7/Adr tumor bearing nude mice (DOX: 0.15 mg/mL, NPs: 0.2 mg/mL). 24 h later, the fluorescence of DOX was detected with live body imaging systems.

In *vivo* Antitumor Assay. For the in *vivo* therapy assay, 50 μL of PBS, DOX, COF, COF(Fe), COF@DOX and COF(Fe)@DOX solutions were intratumorally injected into the MCF-7/Adr tumor bearing nude mice (DOX: 0.15 mg/mL, NPs: 0.2 mg/mL), two days later, another time of drug injection was performed. The tumor growth curves as well as the body weight distribution of different groups were monitored in a 14 d period. To further evaluate the therapeutic effect of different materials, MCF-7/Adr cancer cells were cultured in cell dishes and different materials were co-incubated with the cells for 6 h (PBS, DOX, COF, COF(Fe), COF@DOX and COF(Fe)@DOX, DOX: 0.15 mg/mL, NPs: 0.2 mg/mL). Subsequently, the cells were collected and washed with 1640 medium. Finally, the collected MCF-7/Adr cancer cells were injected into the right axillary region of the nude mice. The tumor formation effect and the body weight changes of the mice in different groups was recorded. For both the two models, at the 4 d during therapy, the main organs of a representative mice from different groups were collected and analyzed by H&E staining.

4. Supplementary data.

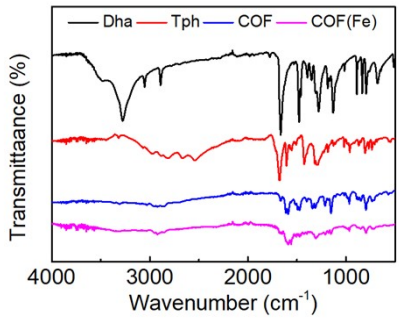

Figure S1. The FT-IR spectra of Dha, Tph, COF, and COF(Fe).

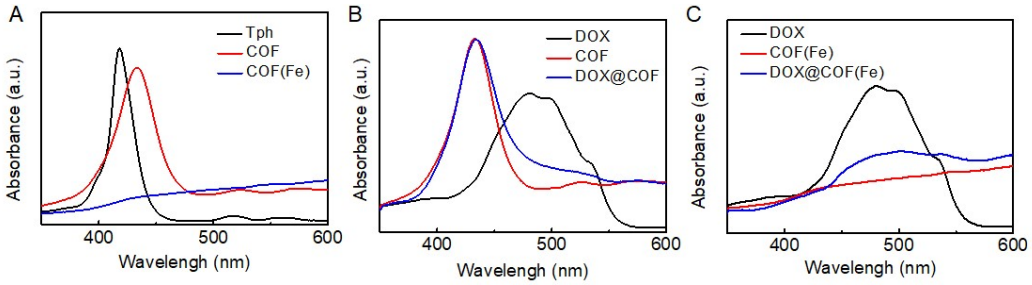

Figure S2. The UV-Vis spectra of Tph, COF, COF(Fe), DOX, DOX@COF and DOX@COF(Fe).

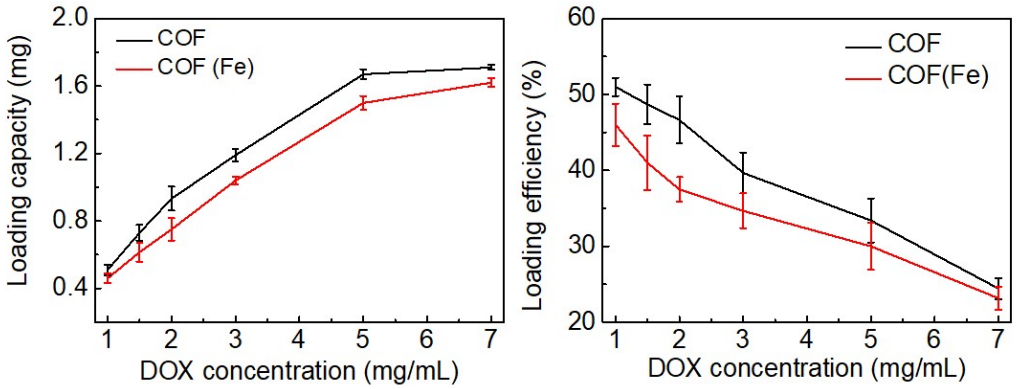

Figure S3. The DOX loading capacities and loading efficiencies of COF and COF(Fe) under different DOX concentrations.

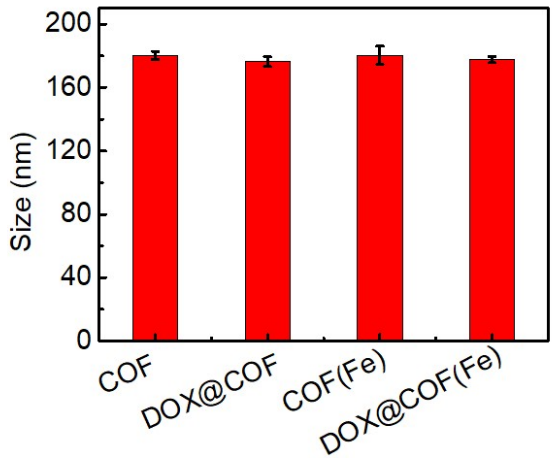

Figure S4. The average size of COF, DOX@COF, COF(Fe) and DOX@COF(Fe).

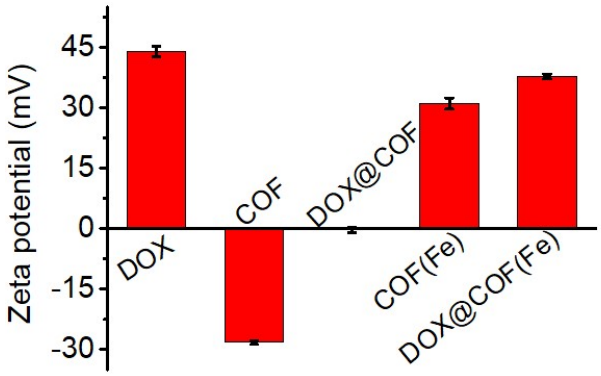

Figure S5. The zeta potential of DOX, COF, DOX@COF, COF(Fe) and DOX@COF(Fe).

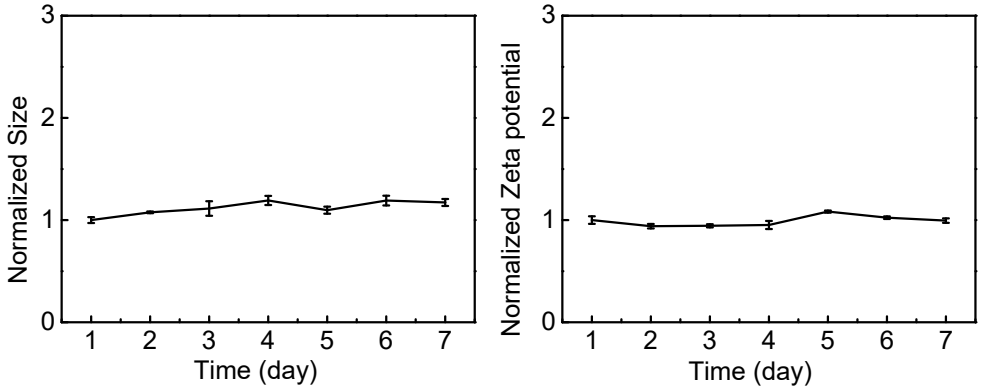

Figure S6. The normalized size and surface zeta potential of COF(Fe) NPs during storage in PBS solution for 7 days.

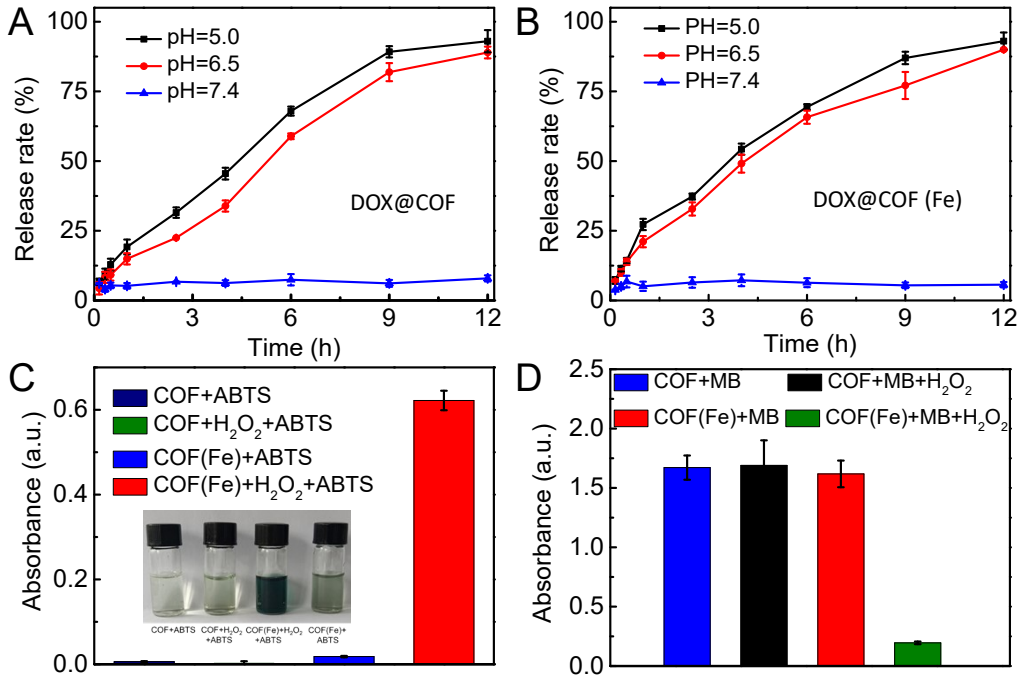

Figure S7. Drug release profiles of (A) DOX@COF and (B) DOX@COF(Fe) solutions with different pH values. (C) The absorption intensity of ABTS at 740 nm with different treatments. Insert is the photographs of the solutions with diverse conditions. (D) The absorption intensity of MB at 668 nm with different treatments

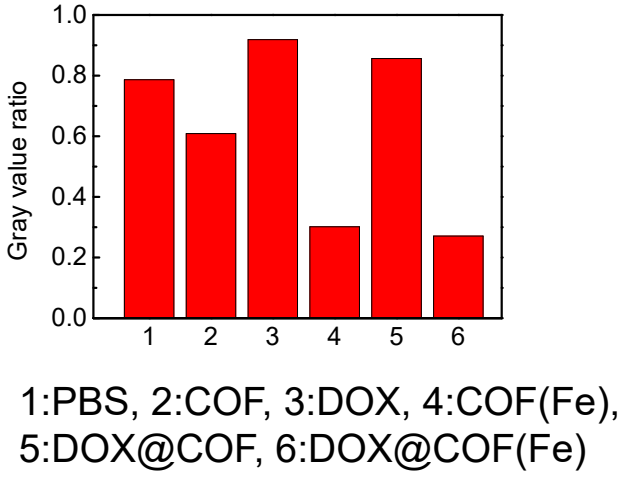

Figure S8. Quantitative analysis of intracellular P-gp expression in MCF-7/Adr cancer cells after different treatments.

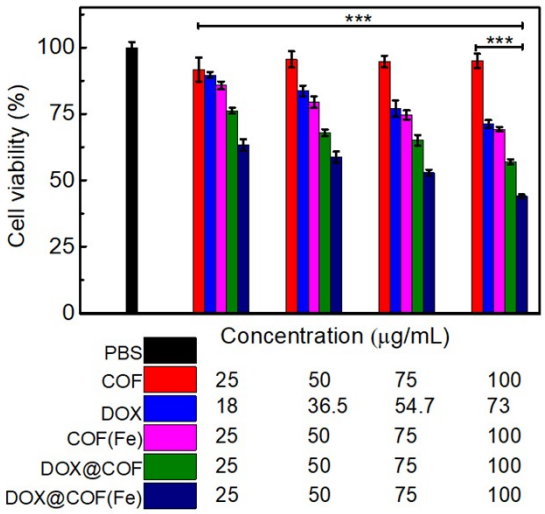

Figure S9. Cell viabilities of MCF-7/Adr cancer cells with different treatments.

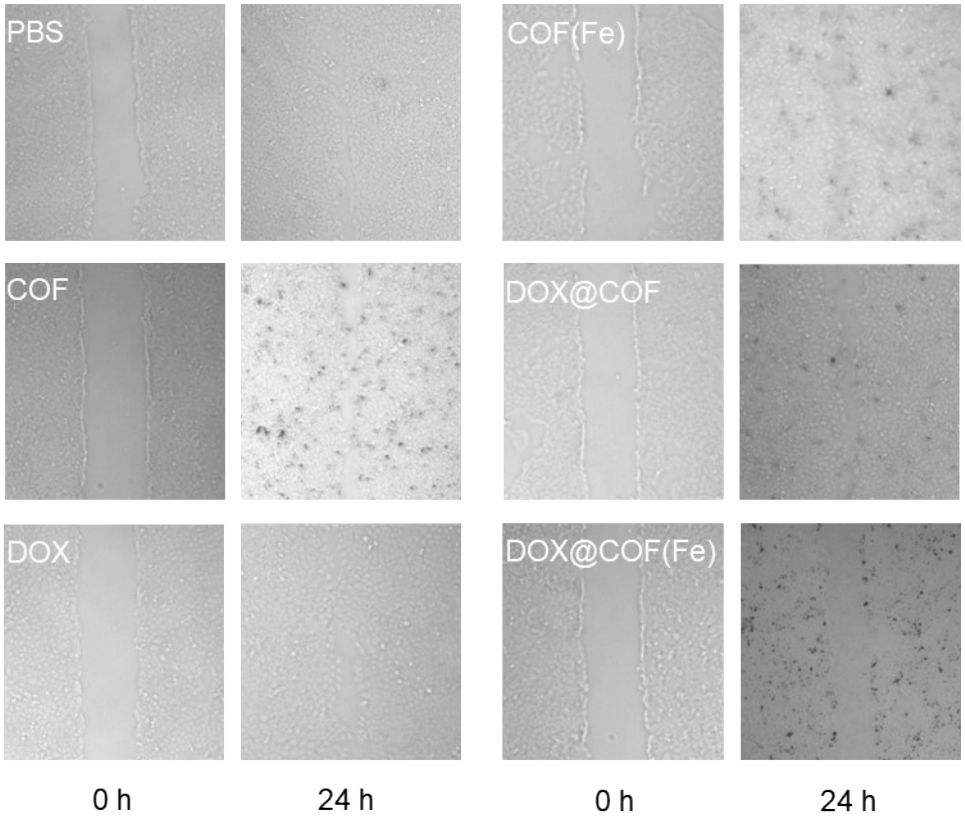

Figure S10. Wound-healing assay of cells received with different treatments at 0 and 24 h.

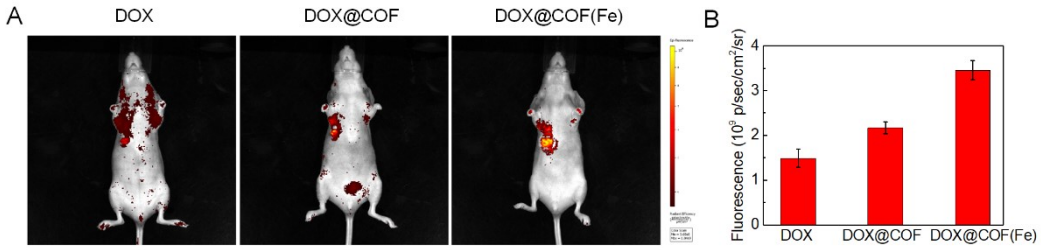

Figure S11. (A) In vivo fluorescence imaging of DOX in tumor bearing nude mice injected with different drugs in the tumor sites post 24 h. (B) The relative fluorescence intensities of DOX at the tumor region in (A).

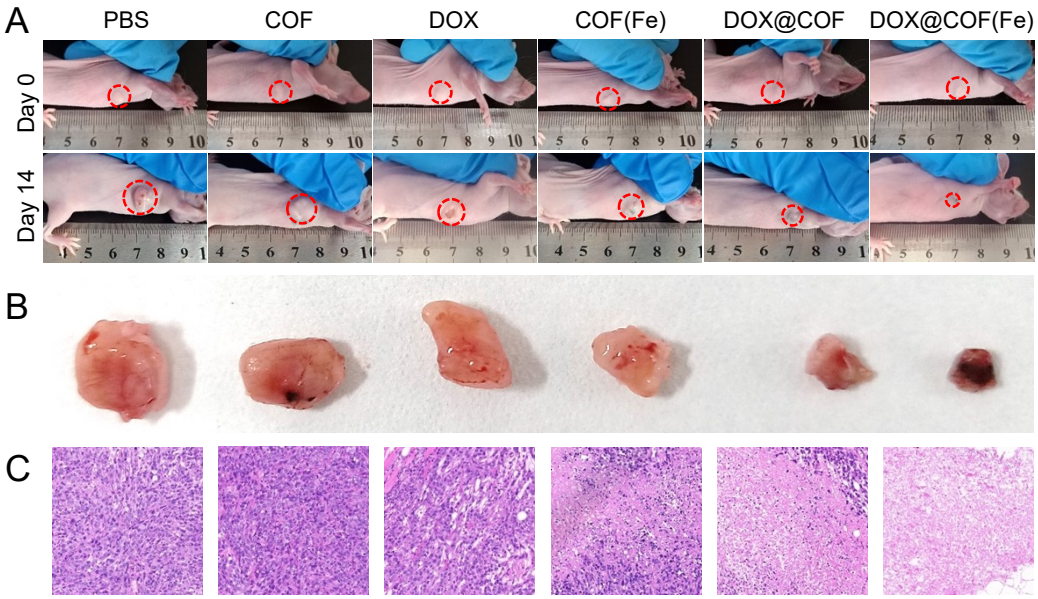

Figure S12. (A) Photographs of tumor bearing nude mice at day 0 and day 14 with different treatments. (B) Representative tumor photograph on the day 14 from different groups in (A). (C) H&E staining of tumor tissues at day 4 receiving different treatments. Magnification, 20×.

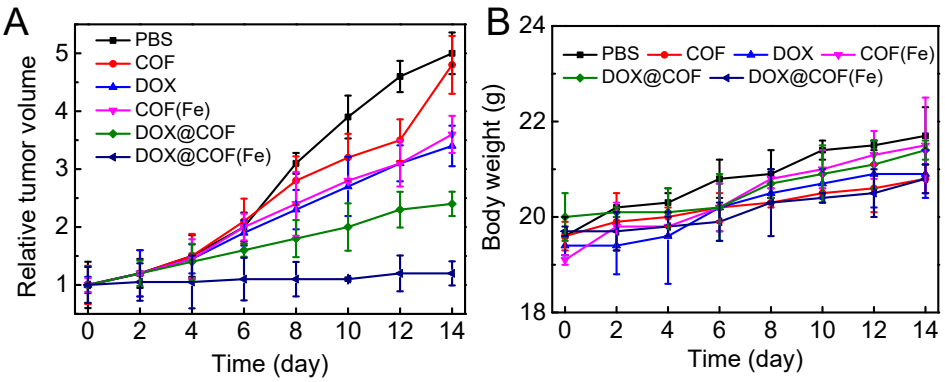

Figure S13. (A) The relative tumor growth curves and (B) body weight changes in different treatment groups within 14 days.

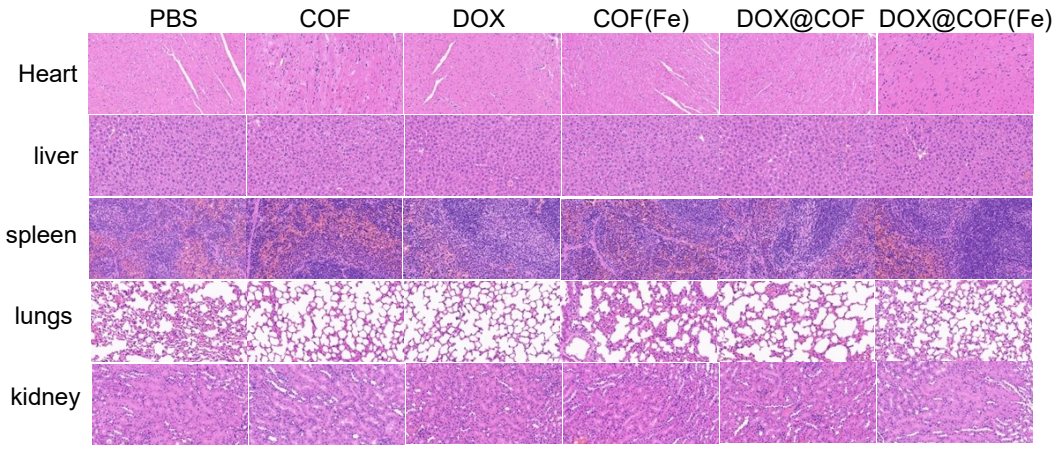

Figure S14. H&E staining of main organs of mice in different groups in the in vivo tumor formation model. Magnification, 20×.

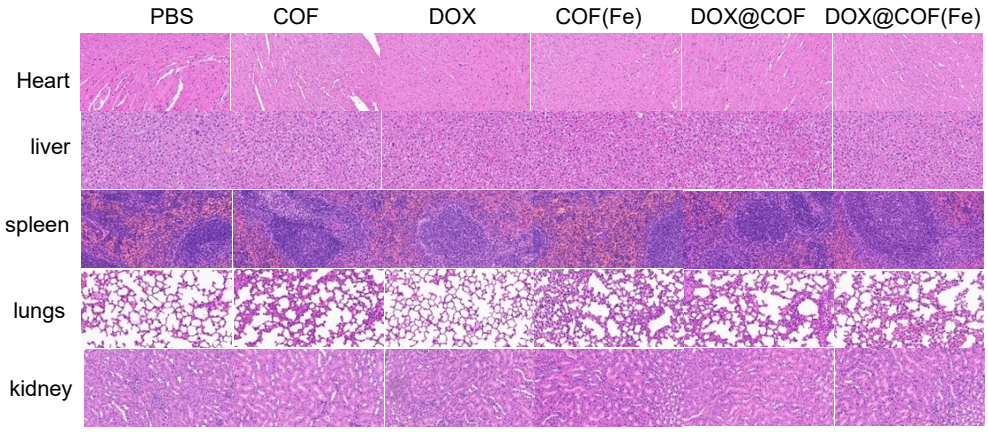

Figure S15. H&E staining of main organs of mice in different groups in the in vivo solid tumor therapy model. Magnification, 20×.

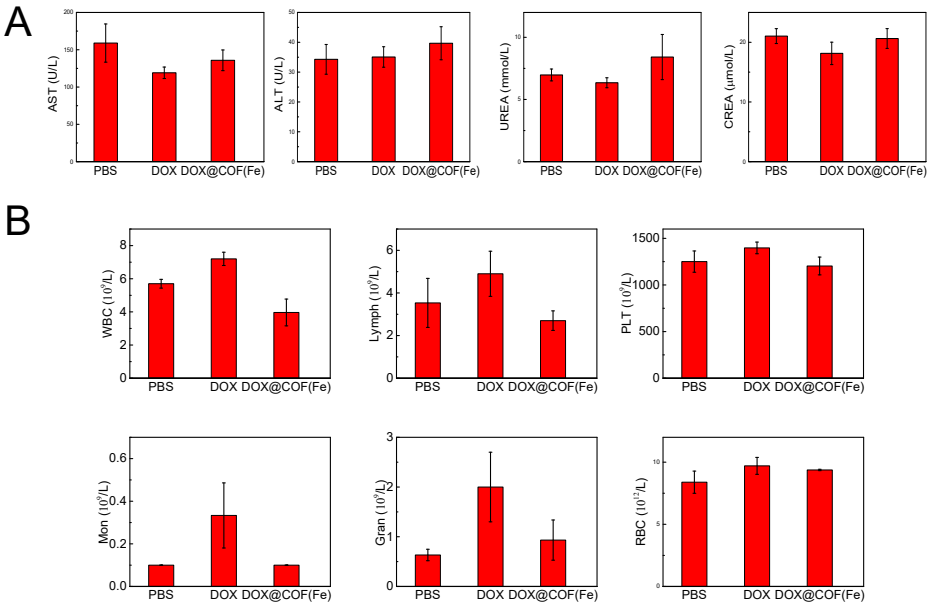

Figure S16. The results of (A) serum biochemistry and (B) blood routine tests of mice intratumorally injected with DOX or DOX@COF(Fe), PBS was employed as the control.